PERFORMANCE ANALYSIS OF MRC-SC MACRODIVERSITY RECEPTION OVER GENERALIZED FADING CHANNELS

UDC (621,395,38:519.724)

Nenad Milošević, Dejan Milić, Daniela Milović, Jelena Anastasov

University of Niš, Faculty of Electronic Engineering,
Department of Telecommunications, Republic of Serbia

Abstract. *This paper shows a detailed statistical characterization of a specific system configuration consisting of one multibranch maximal-ratio-combining (MRC) and one selection-combining (SC) micro-level base station, and SC back processing unit at macro level. Primarily, the scenario of the independent and identically distributed generalized-K fading channels is investigated. After that, the correlated branches at SC-based micro-level are assumed. The outage probability and the error probability performance for both cases are defined. According to the presented analytical analysis, numerical results are obtained. Also, the impact of the number of MRC and SC input branches, the impact of the fading/shadowing factor, the predefined outage threshold, the average signal-to-noise ratios and the correlation coefficient on the specified system performance is shown. Simulations validate the accuracy of the proposed analytical analysis.*

Key words: *Micro-diversity, macro-diversity, outage probability, error performance, fading, shadowing*

1. INTRODUCTION

In general, wireless channels are inevitably accompanied by multipath fading and shadowing phenomena effects, which consequently impair the reliability and the overall system performance [1]. Multipath fading arises when a signal propagates over different paths until reaching the destination point [2]. The shadowing phenomenon occurs when large obstacles such as massive hills, buildings, walls, or other objects veil the propagation path of the transmitted signal. In the engineering literature, there are many proposed statistical models that describe fading and shadowing, whether individually or simultaneously. The

gamma-shadowed Nakagami-*m* fading i.e., generalized-*K* fading distribution has been proposed in [3], [4] as quite general composite model to define the simultaneous effects of fading and shadowing.

Over the years, problems caused by fading/shadowing have been addressed in a variety of ways. One of the well-known processing methods is the signal combining [5]. There are spatial, time, frequency, and polarization diversity schemes. Spatial diversity schemes, micro- and macro-diversity, are more commonly implemented to combat the impact of fading and shadowing, according to the fact that their application does not require the additional transmit power and bandwidth in comparison to other diversity techniques [6]. Furthermore, micro- and macro-diversity are employed to combat the effect of fading and shadowing simultaneously [7]-[11].

In the selection-combining (SC) scheme, a receiver selects the input branch with the strongest signal and bridges its input to the output. In the maximal-ratio-combining (MRC) technique, the output is formed as a linear combination of the input signals. A better performance is expected to be obtained by the MRC combining scheme in contrast to the SC scheme. In overall, MRC is widely recognized as the optimal combining scheme while the SC receiver is convenient because of its lower complexity and ease of implementation.

In micro-diversity schemes, a number of antennas can be utilized within a single base station with spacing between of an order of a wavelength or even shorter. Thus, micro-diversity antennas can experience different fading conditions and the received signals are usually mutually correlated. Macro-diversity involves the combination signals from two or more base stations that are separated by a certain distance, so the statistical independence of the received signals is easily maintained. In addition, in systems based on the macro-diversity, antennas are positioned at spatially allocated base stations, hence experiencing different shadowing conditions.

A detailed performance analysis in terms of the average channel capacity, the average symbol error probability and the outage probability over composite generalized-*K* fading channels has been obtained in [12]. Authors in [13] have evaluated the level crossing rate and average fade duration at the output of SC type macro-diversity system consisting of two multibranch MRC micro-diversity receivers in the presence of the correlative Nakagami-*m* fading. In [14], the moment generating function-based performance analysis of multibranch MRC diversity receiver over various modulation schemes in the generalized-*K* fading channel has been shown. The utilization of the threshold SC-based macro-diversity to overcome shadowing for outdoor wearable communications has been systematically investigated in [15]. The second order statistics of macro SC based diversity system for radio-frequency vehicle-to-infrastructure communications over interference limited fading environment have been shown in [16].

In this paper, we consider the standard MRC processing and so the general form of the receiver output and the initial steps in the performance evaluation are well-known. However, the macro-diversity layout creates a new channel structure which is far more complex than the micro-diversity channel. Hence, the MRC output has a completely new statistical distribution and a novel, more advanced analysis is required for a system performance evaluation. In particular, we consider a combining configuration with multibranch MRC and multibranch SC micro- and SC macro-level combining hierarchy over independent and identically distributed (i.i.d.) fading channels. Generalization to independent *M*-branch MRC and correlated two-branch SC micro level scenario is also presented in this paper. The outage and system error performance have been investigated

for these specific scenarios. In comparison to the works presented in [12]-[14], the system under consideration in our paper has a higher level of complexity, involving the MRC combining at micro-level. Also, a detailed analysis is performed assuming quite general shadowed fading channels, generalized-*K* fading channels, even when the input branches at macro-level receiver are correlated. For an uncorrelated scenario, the analysis is extended for the system configuration when micro-level receivers are equipped by multiple antennas.

In Section 2 the system model under consideration is explained and an equivalent non-hierarchical logical schematic of configuration is shown. A statistical analysis of *M*-branch MRC and *N*-branch i.i.d. micro level scenario, as well as the analysis of the correlated two-branch SC micro level scenario is given in Subsection 2.1. The expressions for the outage probability and average bit error rate (BER) analysis for both scenarios are derived in Subsection 2.2. In order to accomplish high generality of presented analytical analysis, the composite generalized-*K* fading channels were assumed. Numerical results and a discussion are indicated in Section 3 and final concluding remarks are listed in Section 4.

2. PROBLEM FORMULATION

The system model under consideration is shown in Fig. 1. In order to increase the coverage area and to avoid the influence of interferences, base stations (BSs) are allocated in such manner to be closer to each other with the capability to individually cover shorter ranges. Consequently, in the uplink wireless communication in Fig 1, the two nearest BSs can receive copies of the same signal from a mobile station (MS). We assume that one of the BSs is equipped with an MRC microreceiver, while the other BS uses a simpler SC microreceiver. Therefore, there is no need to assume that all BSs are identical, which in turn enables an analysis even in more complex networks of heterogeneous nature. The received signals from both BSs are further processed in the back processing unit (BPU).
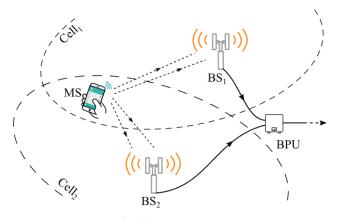

Fig. 1 System model

Simplification of this system model in terms of MRC and SC blocks is given in Fig 2. The input signals of the MRC microreceiver are x_1 and x_2, while the input signals of the SC micro-diversity antennas are x_3 and x_4, respectively. Also, the signal-to-noise ratio (SNR) parameters exist as signal quality measures and input factors for further analysis. The SNR is

a measure that compares the useful signal level to the noise level. The SNRs at the inputs of the MRC microreceivers are γ_1 and γ_2, while the SNR at its output is denoted as γ_5. SNRs at the input of the SC and equivalently – at the inputs of macro level combiner are γ_3 and γ_4, respectively. These three SNRs, γ_5, γ_3 and γ_4, are simultaneously inputs to an equivalent SC macroreceiver (see Fig. 3). Namely, the two 2:1 SCs can be replaced with one equivalent 3:1 SC without affecting the operation of the overall receiving system. Output of the SC macroreceiver located at BPU has a resulting signal whose SNR is denoted as γ_6.

The standard way of analysis concentrates on probability density functions (pdfs) at the output of micro level combiners [7], [8], [13] and continues in the same hierarchical manner to the macro level and its output. Depending on the fading statistics and type of combiners used, an analysis can be tricky and can lead to significant mathematical complexity. The proposed equivalent combiner approach enables a more elegant analysis without compromising the accuracy of the obtained results.
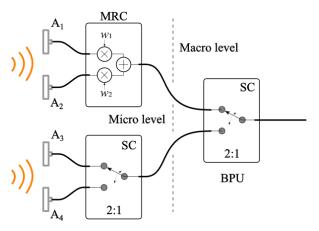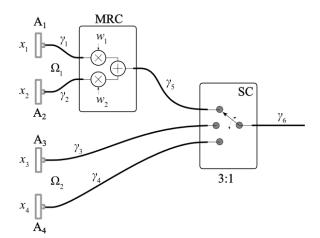

Fig. 2 Combining configuration with micro- and macro-level combining hierarchy

Fig. 3 Equivalent non-hierarchical logical schematic of configuration from Fig. (2). The two 2:1 SCs are replaced with one 3:1 SC.

2.1. Proposed approach in statistic analysis

Macro-level combiner switches the input with highest SNR value to its output, so the output SNR can be expressed as

$$\gamma_6 = \max(\gamma_3, \gamma_4, \gamma_5) \tag{1}$$

Using the conditional probability, the pdf of the output SNR value can be derived as [12]

$$p_{\gamma_6}(x) = p_{\gamma_3}(x)F_{\gamma_4}(x)F_{\gamma_5}(x) + p_{\gamma_4}(x)F_{\gamma_3}(x)F_{\gamma_5}(x) + p_{\gamma_5}(x)F_{\gamma_3}(x)F_{\gamma_4}(x) \tag{2}$$

where $F(\cdot)$ designates the cumulative distribution function (cdf). We assume that signals x_3 and x_4 are mutually independent and identically distributed (i.i.d.), so their pdfs and cdfs are $p_{\gamma_{3/4}}(x)$, and $F_{\gamma_{3/4}}(x)$, respectively. Therefore, we rewrite the previous equation as

$$p_{\gamma_6}(x) = p_{\gamma_5}(x)F_{\gamma_{3/4}}^2(x) + 2p_{\gamma_{3/4}}(x)F_{\gamma_{3/4}}(x)F_{\gamma_5}(x) \tag{3}$$

The interesting configuration of this system enables us to formulate the following lemma:

Lemma 1. When the mentioned cdfs of input signals are expressed in a closed form, and are continuously differentiable, then also the resulting pdf at the ouput of macro-level combiner is expressed in a closed form. The same stands for the cdf of output signal.

Proof. Pdfs are already expressed in a closed form, following from the previous derivation. We now proceed to prove this for cdfs also. By definition, the cdf is $F_{\gamma_6}(x) = \int_{-\infty}^{x} p_{\gamma_6}(t)dt$, and for the specified case it transforms into

$$F_{\gamma_6}(x) = \int_{-\infty}^{x} p_{\gamma_5}(t)F_{\gamma_{3/4}}^2(t)dt + 2\int_{-\infty}^{x} p_{\gamma_{3/4}}(t)F_{\gamma_{3/4}}(t)F_{\gamma_5}(t)dt \tag{4}$$

We proceed with integration by parts on the first addend, taking $u(x) = F_{\gamma_{3/4}}^2(x)$, and $dv(x) = p_{\gamma_5}(x)dx$. It follows that $du(x) = 2F_{\gamma_{3/4}}(x)p_{\gamma_{3/4}}(x)$ and $v(x) = F_{\gamma_5}(x)$. Then the integral can be rewritten as

$$\int_{0}^{x} p_{\gamma_5}(t)F_{\gamma_{3/4}}^2(t)dt = (F_{\gamma_{3/4}}^2(t)F_{\gamma_5}(t))\Big|_{0}^{x} - 2\int_{0}^{x} p_{\gamma_{3/4}}(t)F_{\gamma_{3/4}}(t)F_{\gamma_5}(t)dt \tag{5}$$

We have used the property $p_{\gamma_{3/4}}(x) = 0$ for $x \leq 0$ to replace the lower limit of integration $-\infty$ with 0.

We notice that the second addend conveniently cancels out with the opposite sign addend form (4). Consequently, we can directly write the resulting cdf in symbolic form as

$$F_{\gamma_6}(x) = F_{\gamma_{3/4}}^2(x)F_{\gamma_5}(x) . \tag{6}$$

The result does not depend on the specific type of combiner used in the upper arm, and applies to arbitrary combining technique in this arm, as long as the cdf function of its output is continuously differentiable, as is the case in the majority of fading models.

Corollary 1.1. Single 2:1 SC combiner is obtained when $x_1 = x_2 = 0$. Then $p_5(x) = \delta(x)$ is simply a Dirac δ-function, and $F(x) = h(x)$ is a Heaviside step-function. Then the 3:1 combiner acts as a simple 2:1 combiner with inputs x_3 and x_4. Using (6), the cdf function
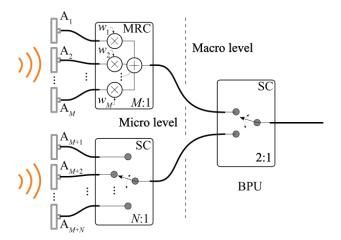
at its output is $F(x) = F_{\gamma_{3/4}}^2(x)$, whereas the pdf is simply its derivative: $p_6(x) = \mathrm{d}F(x)/\mathrm{d}x$ $= 2p_{\gamma_{3/4}}(x)F_{\gamma_{3/4}}(x)$.

Corollary 1.2. The 3-inputs SC combiner results are obtained when $p_5(x) = p_{\gamma_{3/4}}(x)$, and $F(x) = F_{\gamma_{3/4}}(x)$. Then the 3:1combiner acts on three i.i.d. signals yielding output $F(x) = F_{\gamma_{3/4}}^3(x)$, and $p_6(x) = 3p_{\gamma_{3/4}}(x)F_{\gamma_{3/4}}^2(x)$.

Corollary 1.3. Using the previous two corollaries, it recursively follows that an *N*-input SC combiner yields $F(x) = F_{\gamma_{3/4}}^N(x)$, and $p_6(x) = Np_{\gamma_{3/4}}(x)F_{\gamma_{3/4}}^{N-1}(x)$.

Corollary 1.4. SC macro-diversity using an *M*-input MRC micro-diversity and an *N*-input SC micro-diversity: It follows that the output cdf is $F(x) = F_{\gamma_{3/4}}^N(x)F_{\gamma_5}(x)$, whereas pdf is $p_6(x) = p_{\gamma_5}(x)F_{\gamma_{3/4}}^N(x) + Np_{\gamma_{3/4}}(x)F_{\gamma_{3/4}}^{N-1}(x)F_{\gamma_5}(x)$. Here γ_5 refers to SNR at the output of the *M*-branch MRC micro combiner.

Remark 1.1. Results also apply to a case where signals x_3 and x_4 (see Fig. 3) are coming from outputs of two separate micro combiners of an arbitrary type, that are subjected to i.i.d. fading at an earlier combining stage.

Fig. 4 More general combining configuration with *M*-branch MRC and *N*-branch SC at micro level, corresponding to corollary 1.4.

Lemma 2. Generalization to non-i.i.d. signals at individual BSs.
Proof. Let us assume that the signals at the two base stations are uncorrelated. On the other hand, signals at each antenna on any particular base station may be correlated, and thus non-independent, and also possibly non-i.i.d. In that case, referring to Fig. 3, we can describe signal statistics using joint pdfs and cdfs $p_{\gamma_3\gamma_4}(x,y)$, and $F_{\gamma_3\gamma_4}(x,y)$, respectively. The output SNR is then defined as

$$p_{\gamma_6}(x) = p_{\gamma_3}(x)P(\gamma_4, \gamma_5 < x) + p_{\gamma_4}(x)P(\gamma_3, \gamma_5 < x) + p_{\gamma_5}(x)P(\gamma_3, \gamma_4 < x), \qquad (7)$$

where $p_{\gamma_3}(x)$ and $p_{\gamma_4}(x)$ are marginal pdfs of the joint pdf with respect of subscript random variable, and $P(x, y < z)$ represents probability that realizations of random variables x and y are both lower than value z. Using the joint pdf, we can rewrite the previous equation as

$$p_{\gamma_6}(x) = F_{\gamma_5}(x)\int_0^x p_{\gamma_3\gamma_4}(x,t)\mathrm{d}t + F_{\gamma_5}(x)\int_0^x p_{\gamma_3\gamma_4}(s,x)\mathrm{d}s + p_{\gamma_5}(x)\int_0^x\int_0^x p_{\gamma_3\gamma_4}(s,t)\mathrm{d}s\mathrm{d}t \ . \tag{8}$$

The cdf at the output of macro-diversity is

$$F_{\gamma_6}(x) = \int_0^x\int_0^y F_{\gamma_5}(y)p_{\gamma_3\gamma_4}(y,t)\mathrm{d}t\mathrm{d}y + \int_0^x\int_0^y F_{\gamma_5}(y)p_{\gamma_3\gamma_4}(s,y)\mathrm{d}s\mathrm{d}y$$

$$+\int_0^x\int_0^y\int_0^y p_{\gamma_5}(y)p_{\gamma_3\gamma_4}(s,t)\mathrm{d}s\mathrm{d}t\mathrm{d}y. \tag{9}$$

We proceed with analyzing the last addend, via the use of integration by parts. We use $u = \int_0^y\int_0^y p_{\gamma_3\gamma_4}(s,t)\mathrm{d}s\mathrm{d}t$, and $\mathrm{d}v = p_{\gamma_5}(y)\mathrm{d}y$, yielding $\mathrm{d}u = \mathrm{d}y\left(\int_0^y p_{\gamma_3\gamma_4}(s,y)\mathrm{d}s + \int_0^y p_{\gamma_3\gamma_4}(y,t)\mathrm{d}t\right)$ and $v = F_{\gamma_5}(y)$. Then we get

$$\int_0^x p_{\gamma_5}(y)F_{\gamma_3\gamma_4}(y,y)\mathrm{d}y = \left(F_{\gamma_5}(y)F_{\gamma_3\gamma_4}(y,y)\right)\Big|_0^x$$

$$-\int_0^x\mathrm{d}y\left[F_{\gamma_5}(y)\left(\int_0^y p_{\gamma_3\gamma_4}(s,y)\mathrm{d}s + \int_0^y p_{\gamma_3\gamma_4}(y,t)\mathrm{d}t\right)\right] \tag{10}$$

After canceling the addends with opposite signs in (9) and (10), the final result is

$$F_{\gamma_6}(x) = F_{\gamma_5}(x)F_{\gamma_3\gamma_4}(x,x) \ . \tag{11}$$

2.2. Performance analysis at micro and macro-level over generalized-K fading channels

In the system under consideration, we assume that radio channels are corrupted by the composite generalized-K fading due to presence of simultaneous effects of the multipath fading and shadowing. Micro-diversity basic application purpose is to diminish influences of aforementioned channel phenomena, which justifies the assumption regarding the fading channel and even shows the generality of derived equations according to the generality of the generalized-K distribution. Further, mitigation of shadowing requires the use of macro-diversity.

Let the fading envelope over the l-th branch be described by the generalized-K random variable, r_l, following the probability density function (pdf) as [3]

$$p_{R_l}(x) = \frac{4x^{k_l+m_l-1}}{\Gamma(m_l)\Gamma(k_l)}\left(\frac{m_l}{k_l}\right)^{\frac{m_l+k_l}{2}} K_{k_l-m_l}\left(2x\sqrt{\frac{m_l}{\Omega_l}}\right), \tag{12}$$

with k_l and m_l determining the shadowing severity sharpness and fading depth, respectively, and $K_c(.)$ being a modified Bessel function of the second kind and the cth order [17, (8.407)]. $\Gamma(\cdot)$ stands for the Gamma function [17].

The pdf of the instantaneous SNR at the input of lth micro-diversity branch can be written in the form [12]

$$p_{\gamma_l}(\gamma) = \frac{2\gamma^{\frac{m+k-2}{2}}}{\Gamma(m)\Gamma(k)} \left(\frac{mk}{\bar{\gamma}}\right)^{\frac{m+k}{2}} K_{k-m}\left(2\sqrt{\frac{mk\gamma}{\bar{\gamma}}}\right) \tag{13}$$

When $k_l \to \infty$, the generalized-K distribution reduces to the Nakagami-m distribution, and for $k_l \to \infty$ and $m_l = 1$, it reduces to the Rayleigh distribution. For $m_l = 1$, it coincides with K, i.e. the Rayleigh–gamma distribution, and very well approximates the Rayleigh–lognormal distribution. When $k_l \to \infty$ and $m_l \to \infty$, the obtained distribution can describe a channel that is only under the influence of the white Gaussian noise. In addition, the cdf is defined as [12]

$$F_\gamma(\gamma) = \frac{1}{\Gamma(m)\Gamma(k)} G_{1,3}^{2,1}\left(\frac{mk\gamma}{\bar{\gamma}} \left| \begin{matrix} 1 \\ k,m,0 \end{matrix}\right.\right). \tag{14}$$

In order to study the outage probability and the average bit error rate (BER) of the overall system, the cdf of SNRs at the output of MRC and SC receivers will be obtained.

The pdf of SNR at the M-branch MRC output can be calculated as [14]

$$p_{\gamma_{mrc}}(\gamma) = 2\frac{\gamma^{\frac{mM+k}{2}-1}}{\Gamma(mM)\Gamma(k)} \left(\frac{mk}{\bar{\gamma}}\right)^{\frac{mM+k}{2}} K_{k-mM}\left(2\sqrt{\frac{mk\gamma}{\bar{\gamma}}}\right). \tag{15}$$

Further, the cdf of γ_{mrc} can be obtained by transforming the Bessel K function into the Meijer's G function [19] and utilizing [20], in the following way

$$F_{\gamma_{mrc}}(s) = \frac{1}{\Gamma(mM)\Gamma(k)} \left(\frac{mk\gamma}{\bar{\gamma}}\right)^{\frac{mM+k}{2}} G_{1,3}^{2,1}\left(\frac{mk\gamma}{\bar{\gamma}} \left| \begin{matrix} 1-\dfrac{mM+k}{2} \\ \dfrac{k-mM}{2}, \dfrac{mM-k}{2}, -\dfrac{k+mM}{2} \end{matrix}\right.\right). \tag{16}$$

In the case of presence of correlation among branches, the expressions should be modified. According to the fact that the bivariate pdf of the input correlated SNRs over generalized-K fading channels, can be evaluated as [18]

$$p_{\gamma_1\gamma_2}(\gamma_1,\gamma_2) = \frac{4}{\Gamma(m)\Gamma(k)} \sum_{a,b=0}^{\infty} \frac{\rho_n^a}{a!\Gamma(m+a)} \frac{\rho_g^b}{b!\Gamma(k+b)}$$

$$\frac{\prod\limits_{\ell=1,2}\left(mk\dfrac{\gamma_\ell}{\sqrt{\bar{\gamma}_\ell}}\right)^\xi K_\psi\left(2\sqrt{mk\dfrac{\gamma_\ell}{\sigma_\ell}}\right)}{\gamma_1\gamma_2(1-\rho_n)^{k+a+b}(1-\rho_g)^{m+a+b}}, \tag{17}$$

where $\xi = k+m+a+b$, $\psi = k+b-m-a$, $\sigma_{\gamma_l} = (1-\rho_n)(1-\rho_g)\bar{\gamma}_l$, with ρ_n and ρ_g being correlation parameters. In this section, we analyse the case of an independent M-branch MRC and a correlated two-branch SC micro level scenario. Thus, the bivariate cdf of two correlated generalized-K SNRs is defined as [18]

$$F_{\gamma_1\gamma_2}(\gamma_1,\gamma_2) = \frac{1}{\Gamma(m)\Gamma(k)(1-\rho_g)^m(1-\rho_n)^k}$$

$$\sum_{a,b=0}^{+\infty} \frac{\rho_n^a}{a!\Gamma(m+a)} \frac{\rho_g^b}{b!\Gamma(k+b)} \frac{1}{((1-\rho_g)(1-\rho_n))^{a+b}} \qquad (18)$$

$$\prod_{\ell=1,2} \left(\frac{mk\gamma_\ell}{\bar{\gamma}_\ell}\right)^{\xi/2} G_{1,3}^{2,1}\left(\frac{mk\gamma_\ell}{\sigma_{\gamma_\ell}} \left| \begin{array}{c} 1-\dfrac{\xi}{2} \\ \dfrac{\psi}{2}, -\dfrac{\psi}{2}, -\dfrac{\xi}{2} \end{array} \right.\right).$$

Recalling (6) or (11), the overall outage performance of the system under consideration, can be directly obtained as $P_{out} = F_{\gamma_6}(\gamma_{th})$ for independent i.d. or correlated i.d. branch scenario, respectively, where γ_{th} is the predefined outage threshold. According to the fact that cdf of SNRs at SC and MRC output as well as the cdf of SNR at macro level output are known, we can also evaluate the average BER of the overall system, utilizing

$$P_e = \frac{d^c}{2\Gamma(c)} \int_0^\infty e^{-d\gamma}\gamma^{c-1}F_\gamma(\gamma)\mathrm{d}\gamma , \qquad (19)$$

where the parameters c and d are defined as $(c, d) = (0.5, 1)$ for coherent binary phase-shift-keying (BPSK) and $(c, d) = (0.5, 1)$ for differential BPSK (DBPSK). By substituting (6) or (11) in (18), the system error performance for two specified scenarios can be evaluated.

The previous integral is very complex and easy–to–follow solution, for both uncorrelated/correlated scenarios, cannot be obtained. Thus, we determine the average BER approximated expression, for uncorrelated SC branches, in the range from medium-to-high SNRs, by representing the Meijer's G function in (16), into infinite series [21, eq.(07.34.06.0001.01)]. By substituting (16) and (14) into (6), and then (6) into (19), we solved the integral of three Meijer's G functions, with the help of [21, eq.(07.34.21.0081.01)], in the following form

$$P_e = \frac{d^c\bar{\gamma}}{2mk\Gamma(c)(\Gamma(m)\Gamma(k))^2\Gamma(mM)\Gamma(k)}$$

$$\left[\frac{\Gamma(mM-k)}{k} G_{3,1:1,3:0,1}^{1,2:2,1:1,0}\left(\begin{array}{c} -k,-k-m,-k \\ -k-1 \end{array} \left| \begin{array}{c} 1 \\ k,m,0 \end{array} \right| \begin{array}{c} - \\ 0 \end{array} \left| \frac{mk}{d\bar{\gamma}}, \frac{\bar{\gamma}}{dmk} \right.\right) + \qquad (20)\right.$$

$$\left. \frac{\Gamma(k-mM)}{mM} G_{3,1:1,3:0,1}^{1,2:2,1:1,0}\left(\begin{array}{c} -mM,-mM-m,-mM \\ -mM-1 \end{array} \left| \begin{array}{c} 1 \\ k,m,0 \end{array} \right| \begin{array}{c} - \\ 0 \end{array} \left| \frac{mk}{d\bar{\gamma}}, \frac{\bar{\gamma}}{dmk} \right.\right) \right],$$

with $G_{p,q:p_1,q_1:p_2,q_2}^{m,n:m_1,n_1:m_2,n_2}(\ )$ being the bivariate Meijer's G function [21].

3. NUMERICAL RESULTS

Recalling previously obtained analytical results various numerical results are presented and discussed in this section. In particular, we have analysed the outage probability and the average BER of the system under consideration under different generalized-K fading and shadowing conditions. For the sake of simplicity, results for i.i.d channel conditions are shown, although can be used for evaluating generalized scenarios of correlated and not specifically i.i.d. environmental conditions. All numerical results are accompanied with independent Monte Carlo simulations.

In Fig. 5, the outage probability is plotted as a function of the normalized outage threshold varying number of input branches at macro-diversity SC receiver. The results are evaluated based on corollary 1.4. The increase in number of micro-diversity SC (N) and MRC (M) input branches evidently decreases the outage probability. It can be noticed that the lower values of the outage threshold indicate lower values of outage probability i.e. better system performance, regardless of the number of input branches.
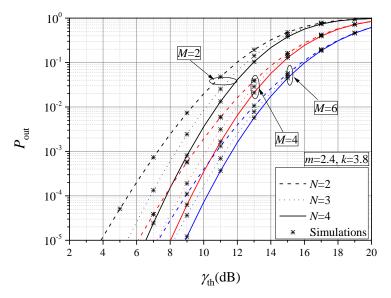

Fig. 5 Outage probability dependence on threshold for uncorrelated scenario

The outage probability dependence on the shadowing shaping factor, k, under various fading conditions is presented in Fig. 6. The outage threshold and number of branches at micro and macro levels remain constant. When fading and/or shadowing parameter increases the outage probability value improves. For higher average SNRs, the impact of fading shaping factor m is more pronounced. For instance, when $k = 2.5$ and the fading depth decreases i.e., m increases from $m = 0.5$ up to $m = 3.5$, the outage probability decreases one order of magnitude for $\bar{\gamma} = 10\text{dB}$ and even three orders of magnitude for $\bar{\gamma} = 15\text{dB}$.
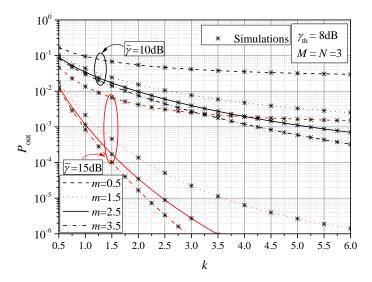
Fig. 6 Outage probability dependence on shadowing shaping factor

Fig. 7 depicts the impact of the average SNR and the fading depth factor (different values of parameter m) on the average BER for two modulation schemes. It can be noticed that the average BER for BPSK signal transmission improves, in comparison to BDPSK signaling. Also, one can notice that changing of the fading depth parameter shows a <u>larger</u> impact on the BDPSK error performance. For instance, by increasing the parameter m from $m=0.5$ to $m=1.5$, when $\bar{\gamma}=16\text{dB}$, the average BER improves for an order of magnitude in the case of DBPSK, and even two orders of magnitude in the case of BDPSK transmission, for the same decrease of fading depth.
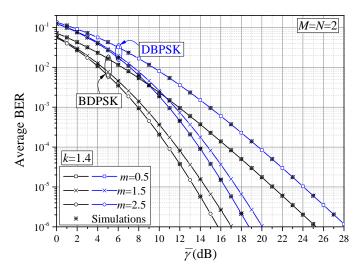

Fig. 7 Average BER versus the average SNR under different fading depth channel conditions
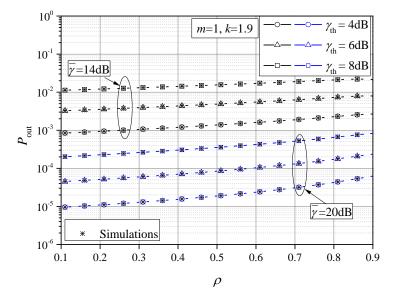
Fig. 8 Outage probability dependence on correlation factor ρ

In Fig. 8, the outage probability dependence on correlation, of the MRC micro level, is shown. The impact of the outage threshold and the average SNR on the outage probability is also depicted. For higher average SNR and/or smaller outage threshold values, better system performance is obtained. It is evident that the correlation coefficient increasing degrades the outage performance. Also, we can notice a more significant influence of correlation coefficient on the outage probability in high SNR regimes (higher slope of blue curves, for $\bar{\gamma} = 20\text{dB}$, is noticeable in comparison to black ones, for $\bar{\gamma} = 14\text{dB}$).

Simulation results show good agreement with analytical results, in all figures.

4. CONCLUSION

In this paper, the outage and error probability performance of a system consisting of MRC and SC receivers at micro- and SC unit at macro-level was investigated. The increase in number of MRC and SC micro-diversity input branches showed to improve the overall system performance. For higher values of fading and/or shadowing parameter, the outage as well as the error performance showed improvement. In the range of higher average SNR values, the impact of fading severity parameter was more pronounced. The average BER improved for the BPSK signal transmission in comparison to BDPSK. For higher average SNR and/or smaller outage threshold values, a better system performance was obtained. Results also showed that the increase in correlation among SC input branches degrades the outage probability values.

REFERENCES

[1] P. M. Shankar, *Fading and Shadowing in Wireless Systems*.Springer Science Business Media, New York, NY, USA, 2012.

[2] H. Suzuki, "A statistical model for urban radio propagation," IEEE Transactions on Communications, vol. 25, no. 7, pp. 673–680, 1977. https://doi.org/10.1109/TCOM.1977.1093888

[3] I. Kostic, "Analytical approach to performance analysis for channel subject to shadowing and fading," IEE Proceedings - Communication, vol. 152, no. 6, pp. 821-827, 2005. https://doi.org/10.1049/ip-com:20045126

[4] P. S. Bithas, N. C. Sagias, P. T. Mathiopoulos, G. K. Karagiannidis and A. A. Rontogiannis, "On the performance analysis of digital communications over generalized-K fading channels," IEEE Communications Letters, vol. 10, no. 5, pp. 353-355, 2006. https://doi.org/10.1109/LCOMM.2006.1633320.

[5] C. B. Dietrich, K. Dietze, J. R. Nealy, and W. L. Stutzman, "Spatial, polarization, and pattern diversity for wireless handheld terminals," IEEE Transactions Antennas Propagations, vol. 49, no. 9, pp. 1271–1281, 2001. https://doi.org/10.1109/8.947018

[6] J. Boutros and E. Viterbo, "Signal space diversity: A power- and bandwidth-efficient diversity technique for the Rayleigh fading channel," IEEE Transactions on Information Theory, vol. 44, no. 4, pp. 1453–1467, 1998. https://doi.org/10.1109/18.681321

[7] A. A. Abu-Dayya and N. C. Beaulieu, "Performance of micro- and macro-diversity on shadowed Nakagami fading channels," in *Proceedings of the IEEE Global Telecommunications Conference GLOBECOM '91: Countdown to the New Millennium. Conference Record*, Phoenix, AZ, USA, pp. 1121-1124 vol.2, 1991, https://doi.org/10.1109/GLOCOM.1991.188549

[8] P. Shankar, "Analysis of microdiversity and dual channel macrodiversity in shadowed fading channels using a compound fading model," AEU - International Journal of Electronics and Communications, vol. 62, no. 6, pp. 445449, 2008. http://dx.doi.org/10.1016/j.aeue.2007.06.008

[9] P. M. Shankar, "Macrodiversity and Microdiversity in Correlated Shadowed Fading Channels," IEEE Transactions on Vehicular Technology, vol. 58, no. 2, pp. 727-732, Feb. 2009. https://doi.org/10.1109/TVT.2008.926622

[10] P. M. Shankar, "Outage Probabilities of a MIMO Scheme in Shadowed Fading Channels with Micro- and Macrodiversity Reception," IEEE Transactions on Wireless Communications, vol. 7, no. 6, pp. 2015-2019, 2008. https://doi.org/10.1109/TWC.2008.070053

[11] D. A. Basnayaka, P. J. Smith, and P. A. Martin, "Performance Analysis of Macrodiversity MIMO Systems with MMSE and ZF Receivers in Flat Rayleigh Fading," IEEE Transactions on Wireless Communications, vol. 12, no. 5, pp. 2240-2251, 2013. http://doi.org/10.1109/TWC.2013.032113.120798

[12] P. S. Bithas, N. C. Sagias, P. T. Mathiopoulos, G. K. Karagiannidis and A. A. Rontogiannis, "On the performance analysis of digital communications over generalized-K fading channels," IEEE Communications Letters, vol. 10, no. 5, pp. 353-355, 2006, https://doi.org/10.1109/LCOMM.2006.1633320.

[13] D. Stefanovic, S. Panic, P. Spalevic, "Second-order statistics of SC macrodiversity system operating over Gamma shadowed Nakagami-m fading channels," AEU - International Journal of Electronics and Communications, vol. 65, no. 5, pp. 413–418, 2011. https://doi.org/10.1016/j.aeue.2010.05.001

[14] V. K. Dwivedi, G. Singh, "Moment Generating Function Based Performance Analysis of Maximal-Ratio Combining Diversity Receivers in the Generalized-K Fading Channels," Wireless Personal Communications, vol. 77, no. 3, pp. 1959–1975, 2014. https://doi.org/10.1007/s11277-014-1618-1

[15] S. K. Yoo, S. L. Cotton, W. G. Scanlon, and G. A. Conway, "An experimental evaluation of switched combining based macro-diversity for wearable communications operating in an outdoor environment," IEEE Transactions on Wireless Communications, vol. 16, no. 8, pp. 5338–5352, 2017. https://doi.org/10.1109/TWC.2017.2709298

[16] C. Stefanovic, S. Veljkovic, M. Stefanovic, S. Panic and S. Jovkovic, "Second Order Statistics of SIR based Macro Diversity System for V2I Communications over Composite Fading Channels," in *Proceedings of the 2018 First International Conference on Secure Cyber Computing and Communication (ICSCCC)*, Jalandhar, India, pp. 569-573, 2018. https://doi.org/10.1109/ICSCCC.2018.8703293

[17] I. S. Gradshteyn, I. M. Ryzhik, *Tables of integrals, series, and products, fifth edition*. Academic Press, New York, USA, 1994.

[18] P. S. Bithas, N. C. Sagias and P. T. Mathiopoulos, "The bivariate generalized-K (K_G) distribution and its application to diversity receivers," *IEEE Transactions on Communications*, vol. 57, no. 9, pp. 2655-2662, 2009. https://doi.org/10.1109/TCOMM.2009.09.080039.

[19] A. P. Prudnikov, Y. A. Brychkov, and O. I. Marichev, *Integrals and Series: Vol. 3: More Special Functions*. CRC Press, New York, NY, USA, 1992.

[20] S. Adamchik and O. I. Marichev, "The algorithm for calculating integrals of hypergeometric type functions and its realization in REDUCE system," in *Proceedings of the International Symposium on Symbolic and Algebraic Computation*, New York, NY, USA, pp. 212–224, 1990. https://doi.org/10.1145/96877.96930

[21] The Wolfarm Functions Site, 2008. [Online] Available: http://functions.wolfram.com/